RESEARCH ARTICLE OPEN ACCESS

Weldability of Friction Welding Process for AA2024 Alloy and SS304 Stainless Steel using Finite Element Analysis

Chennakesava R Alavala
Department of Mechanical Engineering, JNT University, Hyderabad-85

ABSTRACT
The objective of this work was to assess the weldability of AA2024 alloy and SS304 stainless steel. The process parameters were frictional time, frictional pressure, rotational speed and forging pressure. The joints were evaluated for their strength, bulk deformation, penetration and flange formation employing finite element analysis software code. For friction welding of AA2024 alloy and SS304 stainless steel, the ratio of forging pressure / frictional pressure should be optimum for good welding.
***Keywords* -** AA2024 alloy, SS304 stainless steel, frictional time, frictional pressure, rotational speed and forging pressure, friction welding.

I. INTRODUCTION

The difficulties in the welding of aluminum alloy with stainless steel by fusion welding processes have been a great challenge for engineering, because they result from hard and brittle intermetallic phases that are formed between aluminum and steel at elevated temperatures. Joining of a 6-mm thickness Al 6061 to AISI 1018 steel has been performed by the combined effects of fusion and solid state welding. It was found that the intermetallic phases Al_3Fe_4 and Al_5Fe_2 exist in the weld zone [1].

The friction between the surfaces makes possible a rapid temperature rise in the bonding interface, causing the mass to deform plastically and flows depending on the application of pressure and centrifugal force, creating a flash [2-8]. Friction welding of aluminium alloys to copper has been carried under different friction pressures based on the hardness and heat conductivity of each joining aluminium alloy [9]. The effect of rotational speed on interface properties were studied for the AISI 304L to 4340 steel combination [10]. It was found that the width of the fully plastically deformed zone is mainly affected by the rotational speed.

The present work was intended to weld AA2024 aluminum alloy with SS304 stainless steel using friction welding process. The frictional welding was subjected to different conditions of rotational speed, frictional pressure, frictional time and forging pressure. The welding procedure was planned using Taguchi techniques; the frictional welding was modeled using finite element analysis (FEA). The thermo-structural coupled field model was employed to simulate the friction welding process using finite element methods.

II. MATERIALS AND METHODS

Coupled field analysis of thermal and structural was employed to model the friction welding of AA2024 alloy and SS304 using ANSYS WORKBENCH (15.0) software [11]. An axisymmetric 3D model of the AA2024 and SS304 alloys of 25.4 mm diameter and 100 mm length were made using ANSYS workbench as depicted in figure 1. Tetrahedron elements [11] were used to mesh the AA2024 and SS304 alloy rods. For rotation and non-rotating parts, the boundary conditions are shown in figure 2. First the transient thermal analysis was performed keeping the SS304 alloy rod stationary and the AA2024 rod in rotation. The coefficient of friction 0.2 was applied at the inter-face of the AA2024 and SS304 alloy rods. The convection heat transfer coefficient was applied on the surface of two rods. The heat flux calculations were imported from ANSYS APDL commands and applied at the interface of two materials to be welded. The temperature distribution was estimated. The thermal analysis was coupled with the static structural analysis. For the structural analysis the rotating (AA2024) rod was brought to stationary and the forging pressure was applied on the SS304 alloy rod along the longitudinal axis. The SS304 alloy rod was allowed to move in the axial direction. The contact analysis was also carried out to determine the depth of penetration and sliding of the material at the interface. The modeling and analysis of the friction welding was carried out as per the design of experiments using Taguchi techniques. The process parameters and their levels are given table-1. The orthogonal array (OA), L9 was chosen for the present work. Table 2 gives the assignment of parameters to the various columns of OA.

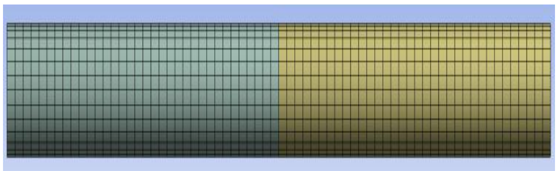

Fig. 1. Finite element modeling of friction welding.

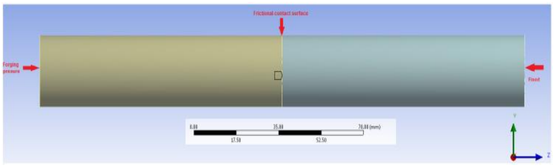

Fig. 2. The boundary conditions.

Table 1. Process parameters and levels

Factor	Symbol	Level–1	Level–2	Level–3
Frictional Pressure, MPa	A	50	60	70
Frictional time, Sec	B	4	5	6
Rotational speed	C	2000	2500	3000
Forging pressure, MPa	D	1.25A	1.50A	1.75A

Table 2. Orthogonal Array (L9) and control parameters

Trial No.	A	B	C	D
1	1	1	1	1
2	1	2	2	2
3	1	3	3	3
4	2	1	2	3
5	2	2	3	1
6	2	3	1	2
7	3	1	3	2
8	3	2	1	3
9	3	3	2	1

III. RESULTS AND DISCUSSION

The statistical Fisher's test was carried out to find the acceptability of process parameters at 90% confidence level.

3.1 Influence of parameters on temperature distribution

Table – 3 presents the ANOVA (analysis of variation) summary of temperature distribution. The frictional pressure (A) and rotational speed (C) would contribute, respectively, 33.90% and 53.22% in the total variation of the welding temperature. The frictional time (B) and forging pressure (D) had very small influence, respectively, of 7.15% and 5.73% on the welding temperature.

Table 3. ANOVA summary of temperature distribution

Source	Sum 1	Sum 2	Sum 3	*SS*	*v*	*V*	*F*	*P*
A	3951.3	4357.6	5065.0	211758.01	1	211758	42351595	33.9
B	4756.8	4310.1	4307.0	44652.28	1	44652	8930454	7.15
C	3809.4	4354.2	5210.3	332470.56	1	332470	66494101	53.22
D	4712.6	6458614.4	13373.9	35793.94	1	35793	7158786	5.73
e				0.02	4	0.005	1.00	0
T	17230.1	6471636.3	27956.2	624674.81	8			100

Note: SS is the sum of square, v is the degrees of freedom, V is the variance, F is the Fisher's ratio, P is the percentage of contribution and T is the sum squares due to total variation.

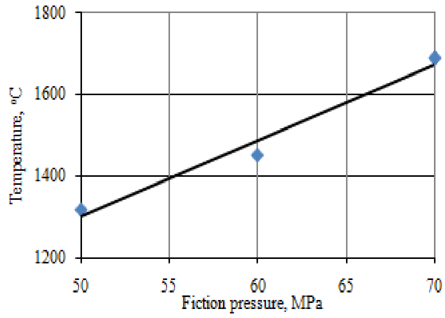

Fig. 3. Influence of frictional pressure on temperature.

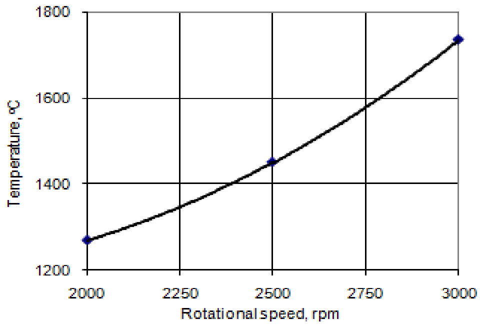

Fig. 4. Influence of rotational speed on temperature.

The temperature was directly proportional to the frictional pressure and rotating speed as shown in figures 3 and 4, respectively. High temperature gradients resulted at the weld interfaces due to high frictional pressure and rotating speed on rods. The welding conditions of trial 7 would generate the highest temperature (2020oC) and trial 2 would produce the lowest temperature (1215oC) in the rods (figure 5).

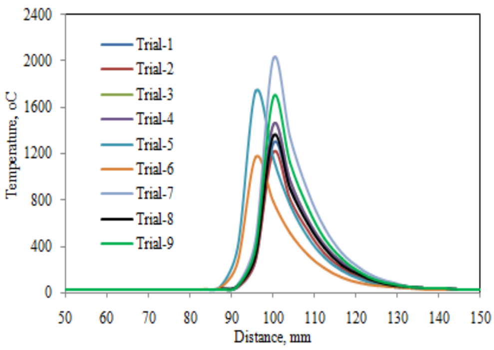

Fig. 5. Temperature distribution during different trials.

3.2 Influence of parameters on equivalent stress

The ANOVA summary of the equivalent stress is given in table 4. The major contributions were attributed to frictional pressure (A), rotational speed (D) and frictional time (B) towards the total variation of effective stress.

Table 4. ANOVA summary of the equivalent stress

Source	Sum 1	Sum 2	Sum 3	SS	v	V	F	P
A	7109.1	7952.0	9268.8	789860.7	1	789860.75	315944366	31.43
B	8945.6	7821.7	7562.6	360330.3	1	360330.33	144132162	14.34
C	6846.0	7907.7	9576.2	1262787	1	1262787.9	505115269	50.24
D	8512.8	21755669.8	24329.9	100460.7	1	100460.72	40184296	4
e				0.01	4	0.0025	1	0
T	31413	21779351.2	50737.50	2513439	8			100

The frictional pressure and rotational speed would enhance the equivalent stress induced in the weld rods as shown in figures 6 and 7. But, the effective stress decreases with the increase of frictional time as shown in figure 8. It can also be observed from figure 9 that the stress induced in the grain refined region of heat affected zone (HAZ) was higher in all the welds than that in the parent metal. The stress induced in the HAZ for trials 7 and 6 were, respectively, 1075 MPa and 470 MPa. The highest and lowest effective stresses were, respectively, 3847 MPa and 2196 MPa induced for trial conditions of 7 and 2 as shown in figure 10.

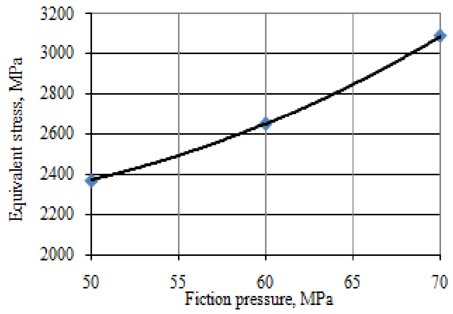

Fig. 6. Influence of frictional pressure on equivalent stress.

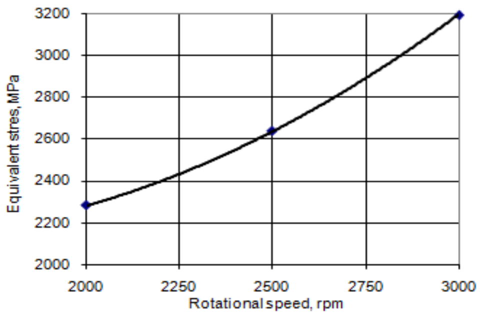

Fig. 7. Influence of rotational speed on equivalent stress.

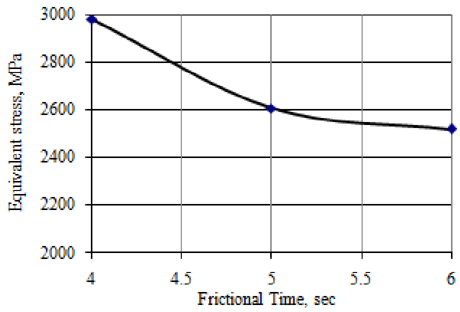

Fig. 8. Influence of frictional time on equivalent stress.

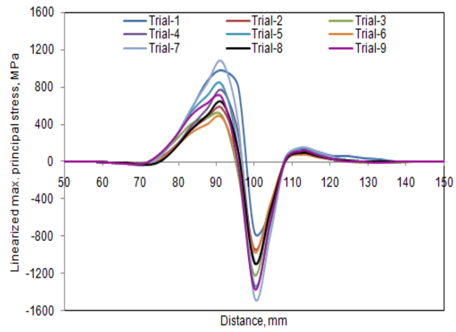

Fig. 9. Linearized maximum principle stress induced in weld rods.

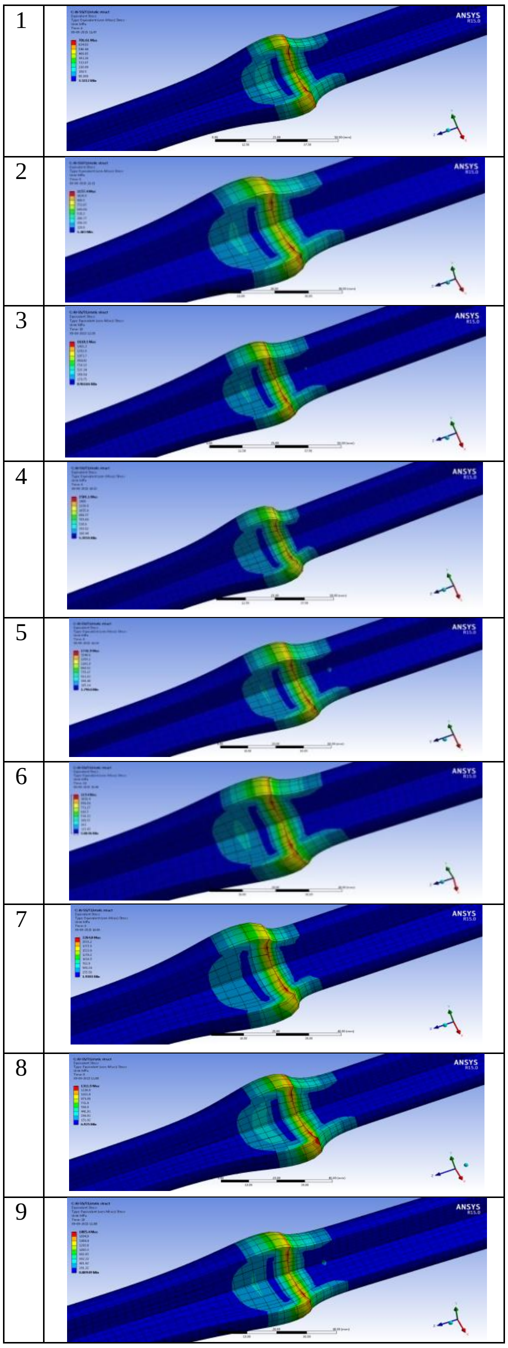

Fig. 10. Equivalent stress values under different trials

3.3 Influence of parameters on bulk deformation

The ANOVA summary of the directional deformation is given in table 5. The major contributions were of frictional time (11.66%), rotational speed (32.61%) and ratio of frictional pressure / forging pressure (64.04%) towards variation in the bulk deformation. The bulk deformation was found to be minimum for 5 sec of frictional time (figure 11). The bulk deformation increased with increase of rotational speed as shown in figure 12. With the increase of forging pressure, the bulk deformation decreased as shown in figure 13 due to compression effect.

Table 5. ANOVA summary of the bulk deformation

Source	Sum 1	Sum 2	Sum 3	SS	v	V	F	P
A	1.54	1.48	1.71	0	1	0	0.00	1.19
B	1.71	1.45	1.58	0.01	1	0.01	8.83	11.66
C	1.48	1.49	1.77	0.03	1	0.03	26.48	32.61
D	1.90	0.74	4.74	0.06	1	0.06	52.96	64.04
e				-0.0045	4	-0.001133	1.00	0.0
T	6.63	5.16	9.80	0.0954	8			100

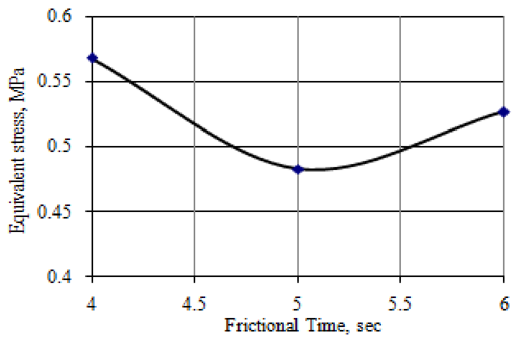

Fig. 11. Influence of frictional time on deformation.

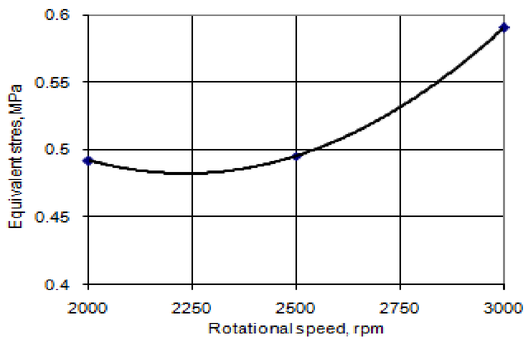

Fig. 12. Influence of rotational speed on deformation.

The extruded shape was asymmetric, as shown in figure 14. The tendency of flange formation was higher with AA2024 than with SS304 stainless steel. The axial shortening on the AA2024 side was more than that on SS304 stainless steel side. Consequently, the AA2024 alloy was moved outward forming the flange at the interface. This is also due to the fact that melting point of AA2024 is lower than that of SS304 stainless steel.

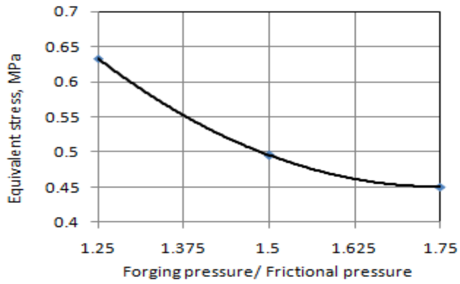

Fig. 13. Influence of ration of forging pressure / frictional pressure on deformation.

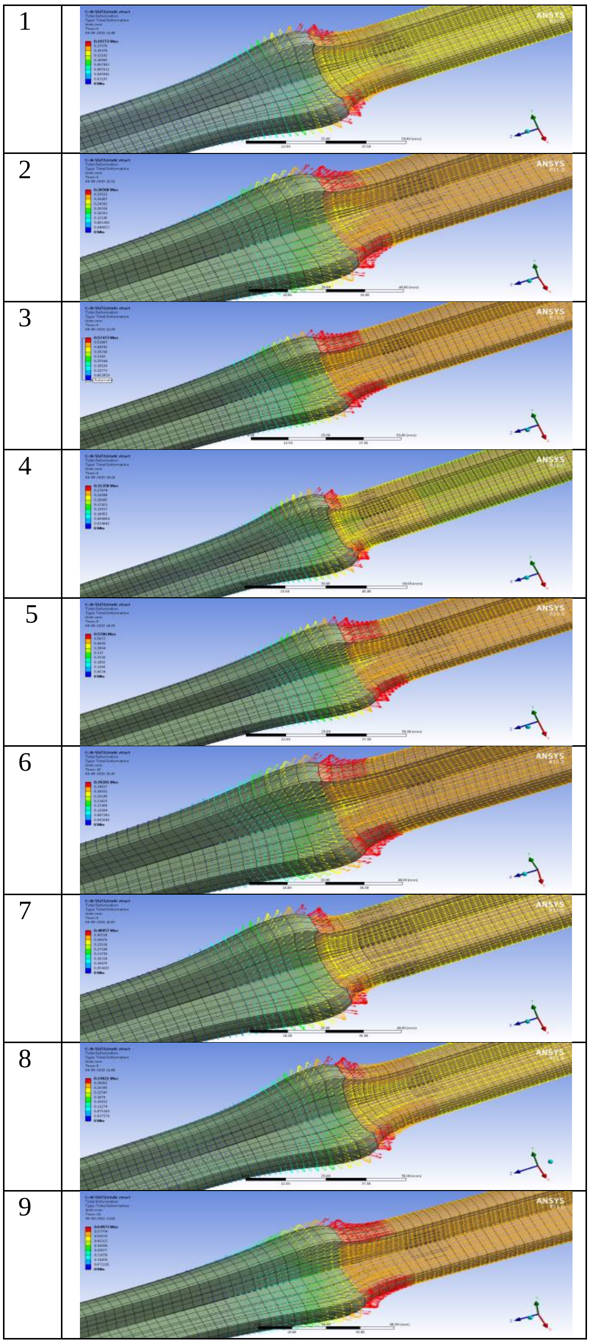

Fig. 14. Bulk deformation values under different trials.

IV. CONCLUSIONS

This study shows that the weldability of AA2024 alloy and SS304 stainless steel is highly dependent on the rotational speed, frictional time and the ratio of forging pressure / frictional pressure. As the stresses induced in the welding rods were very high, it is recommended to relieve them using appropriate heat treatment process.

ACKNOWLEDGEMENTS

The author acknowledges with thanks University Grants Commission (UGC) – New Delhi for sectioning R&D project.

REFERENCES

[1] C. M. Chen, R. Kovacevic, Joining of Al 6061 alloy to AISI 1018 steel by combined effects of fusion and solid state welding, *International Journal of Machine Tools and Manufacture*, 44, 2004, 1205-1214.

[2] V. Srija and A. C. Reddy, Finite Element Analysis of Friction Welding Process for 2024Al Alloy and UNS C23000 Brass, *International Journal of Science and Research*, 4(5), 2015, 1685-1690.

[3] T. Santhosh Kumar and A. C. Reddy, Finite Element Analysis of Friction Welding Process for 2024Al Alloy and AISI 1021 Steel, *International Journal of Science and Research*, 4(5), 2015, 1679-1684.

[4] A. Raviteja and A. C. Reddy, Finite Element Analysis of Friction Welding Process for UNS C23000 Brass and AISI 1021 Steel, *International Journal of Science and Research*, 4(5), 2015, 1691-1696.

[5] A. C. Reddy, Fatigue Life Evaluation of Joint Designs for Friction Welding of Mild Steel and Austenite Stainless Steel, *International Journal of Science and Research*, 4(2), 2015, 1714-1719.

[6] A. C. Reddy, Fatigue Life Prediction of Different Joint Designs for Friction Welding of 1050 Mild Steel and 1050 Aluminum, *International Journal of Scientific & Engineering Research*, 6(4), 2015, 408-412.

[7] A. C. Reddy, Finite Element Analysis of Friction Welding Process for AA7020-T6 and Ti-6Al-4V Alloy: Experimental Validation, *International Journal of Science and Research*, 4(5), 2015, 947-952.

[8] A. C. Reddy, Evaluation of parametric significance in friction welding process for AA2024 and Zr705 alloy using finite element analysis, International *Journal of Engineering Research & Technology*, 5(1), 2016, 84-89.

[9] H. Ochi. et al. Influence of welding conditions on strength of Aluminium alloy to Copper, *Proceedings of the International Offshore and Polar Engineering Conference*, 2001.

[10] Ozdimer. et al., Effect of rotational speed on the interface properties of friction welded AISI 304L to 4340 steel, *Journal of Materials and Design*, 28,2007, 301-307.

[11] C.R. Alavala, Finite Element Methods: Basics Concepts and Applications, *PHI Learning Pvt. Ltd*., New Delhi, 2008.